Bioorganic Chemistry 88 (2019) 102956

Contents lists available at ScienceDirect

Bioorganic Chemistry

journal homepage: www.elsevier.com/locate/bioorg

# Exploration of *N*-alkyl-2-[(4-oxo-3-(4-sulfamoylphenyl)-3,4-dihydroquinazolin-2-yl)thio]acetamide derivatives as anticancer and radiosensitizing agents

Aiten M. Soliman, Mostafa M. Ghorab*

*Department of Drug Radiation Research, National Center for Radiation Research and Technology (NCRRT), Egyptian Atomic Energy Authority (EAEA), Nasr City, P.O. Box 29, Cairo, Egypt*

ARTICLE INFO

*Keywords:*
Quinazolinone
Benzenesulfonamide
Tyrosine kinase
Anticancer

ABSTRACT

Multitargeted therapy is considered a successful approach to cancer treatment. The development of small molecule multikinase inhibitors through hybridization strategy can provide highly potent and selective anticancer agents. A library of *N*-alkyl-2-[(4-oxo-3-(4-sulfamoylphenyl)-3,4-dihydroquinazolin-2-yl)thio]acetamide derivatives **5–18** was designed and synthesized. The synthesized compounds were screened for cytotoxic activity against MDA-MB-231 breast cancer cell line and showed $IC_{50}$ in the range of 0.34–149.10 μM. The inhibition percentage of VEGFR-2 was measured for all the compounds and found to be in the range of 90.09–20.44%. The promising compounds **8, 12, 13, 16** and **17** were selected to measure their possible multikinase inhibitory activity against VEGFR-2 and EGFR. $IC_{50}$ of the promising compounds were in the range of 247–793 nM for VEGFR-2 in reference to sunitinib ($IC_{50}$ 320 nM), and 369–725 nM for EGFR in reference to erlotinib ($IC_{50}$ 568 nM). Compounds **12** and **13** showed the most potent activity towards VEGFR-2 & EGFR, respectively. Measuring the cytotoxicity of **12** and **13** against MCF-10 normal breast cell line indicates their relative safety to normal breast cells ($IC_{50}$ 37 & 97 μM, respectively). As radiotherapy is considered the primary treatment for some types of solid tumors, the radiosensitizing ability of **12** and **13** was measured by subjecting the MDA-MB-231 cells to a single dose of 8 Gy of gamma radiation. $IC_{50}$ of **12** and **13** decreased from 1.91 & 0.51 μM to 0.79 & 0.43 μM, respectively. Molecular docking was performed to gain insights into the ligand-binding interactions of **12** inside VEGFR-2 and EGFR binding sites in comparison to their co-crystallized ligands.

## 1. Introduction

Cancer treatment varies according to the type, stage, possible side effects and the patient's health [1]. Some patients receive one treatment, but most of them require combined therapy including surgery, radiotherapy and chemotherapy. Other therapies may also be required as hormonal, targeted or immunotherapy. Targeted chemotherapy aimed at signaling pathways can provide high efficacy and lower side effects treatment [2]. The use of radiotherapy alone is effective after surgery in case of solid tumors but in case of metastasis, the use of chemotherapy or combined therapy is a must [3,4].

Protein kinases (PKs) are enzymes that phosphorylate a certain amino acid by adenosine triphosphate (ATP), inducing intracellular signal-transduction pathways [5]. PKs are responsible for controlling cell growth, differentiation, cell cycle progression and apoptosis [6]. They are also regarded as the second major promising therapeutic targets after the G-protein coupled receptors and classified according to their substrate specificity into tyrosine and serine-threonine kinases [7]. Tyrosine kinases (TKs) are also divided into receptor and non-receptor TKs [8]. The TK receptors share some common features with slight differences. They consist of an extracellular domain, intracellular domain and a transmembrane region of normal ATP expression range from 40,000 to 100,000 per cell [9]. Deregulation of these kinases is accompanied with cancer development and progression [10].

Protein kinase inhibitors (PKIs) either act by inhibiting autophosphorylation of the kinase or consequent phosphorylation of the protein substrate [11]. The major concern in the development of selective ATP competitive inhibitor is the sequence homology within the ATP binding site [11]. The use of a single small molecule multitargeted TKI able to block multiple signaling pathways has proven to be advantageous to achieve high selectivity, reduced toxicity and drug resistance [2,12,13].

Vascular Endothelial Growth Factor Receptor (VEGFR) and

* Corresponding author.
*E-mail address:* mmsghorab@yahoo.com (M.M. Ghorab).

https://doi.org/10.1016/j.bioorg.2019.102956
Received 23 February 2019; Received in revised form 25 April 2019; Accepted 26 April 2019
Available online 27 April 2019

Epidermal Growth Factor Receptor (EGFR) are members of the receptor tyrosine kinase family (RTK) [14]. VEGFR is considered the secondary target used with the EGFR to design a multikinase inhibitor [12]. VEGF is an important signaling protein responsible for angiogenesis and vascularization [15]. It enhances endothelial cell mitogenesis increasing the permeability of the blood vessels and is up-regulated in tumors [16]. VEGFRIs reduce cancer vascularization and trigger apoptosis. On the other hand, EGFR plays an essential role in cell functions regulations [17]. Its overexpression is more common in solid tumors with poor prognosis and high metastatic rate [18,19]. Patients with mutant EGFR gene are more responsive to EGFR inhibitors as low doses are required for complete suppression of the mutated EGFR signaling [20]. Targeting EGFR can occur either by the use of monoclonal antibodies directed towards the extracellular domain as cetuximab [19,21], or the small molecules inhibitors that inhibit the intracellular domain activity. The most common examples of the latter are the quinazoline-based inhibitors [18].

VEGFR and EGFR share a common hinge region. The structures of their inhibitors are based on 5, 6 or 6, 6 fused bicyclic rings which include a pyrimidine [22,23]. An example of the multitargeted TKIs is sunitinib (Fig. 1). Sunitinib is an oral, type II inhibitor of VEGFR-2, which demonstrated competitive inhibition to ATP. It acts by targeting VEGFR and platelet-derived growth factor receptor b (PDGFRb), thus inhibiting both angiogenesis and cell proliferation [24]. Moreover, Pawar et al. described the quinazolines as the best scaffold to develop an EGFR inhibitor [25]. Examples of quinazolines based inhibitors are lapatinib, erlotinib and afatinib (Fig. 1). Lapatinib is an orally active dual EGFR/HER2 inhibitor that targets breast and lung cancer, while erlotinib and afatinib are EGFR inhibitors, that targets patients with EGFR mutant gene [26].

Hybridization between quinazoline and sulfonamide pharmacophoric cores can provide potent multikinase inhibitors targeting cancerous cell growth and proliferation. The introduction of a sulfonamide group at the N-3 of quinazolinone was reported to increase the EGFR and VEGFR inhibitory activity [27–29]. Besides, sulfonamide is a privileged scaffold that is well known for its anticancer activity by many mechanisms as; matrix metalloproteinase (MMP) inhibition, cyclin-dependent kinase (CDK) inhibition, suppression of the NF-y and carbonic anhydrase (CA) inhibition [30]. Examples of PKIs of sulfonamide origin are the early discovered naphthalene derivative **(A)** [7,31] and fasudil HCl (**B**) that entered clinical trials in 1990 despite its poor selectivity (Fig. 2) [7].

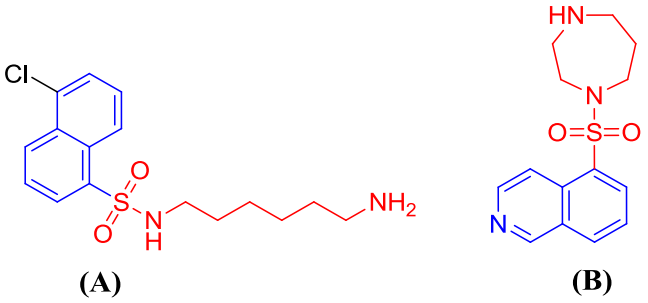


**Fig. 2.** Sulfonamides used as PKIs.

Based on the above, molecular hybridization was utilized between the quinazolinone and benzenesulfonamide followed by grafting different substituents at the acetamide tail to provide a series of varying biological activity. The cytotoxicity of the target compounds was evaluated against cancerous and normal breast cell lines. The dual VEGFR-2/EGFR inhibitory activity and the radiosensitizing effect were

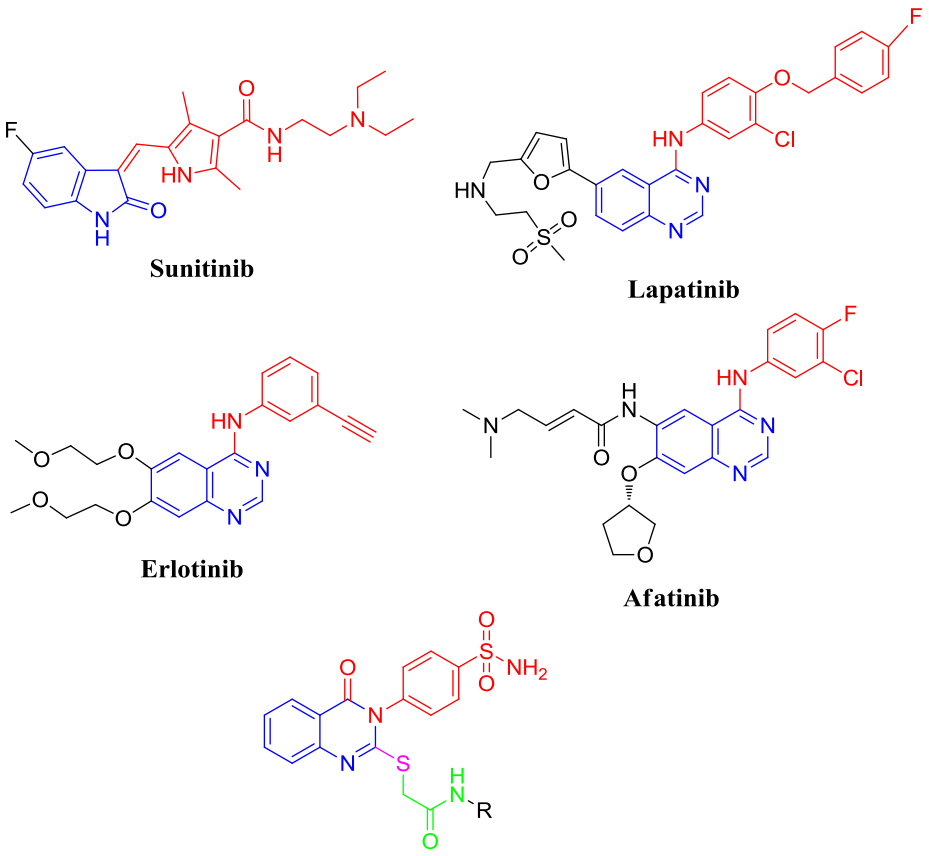


**Fig 1.** Examples of some multitargeted TKIs.

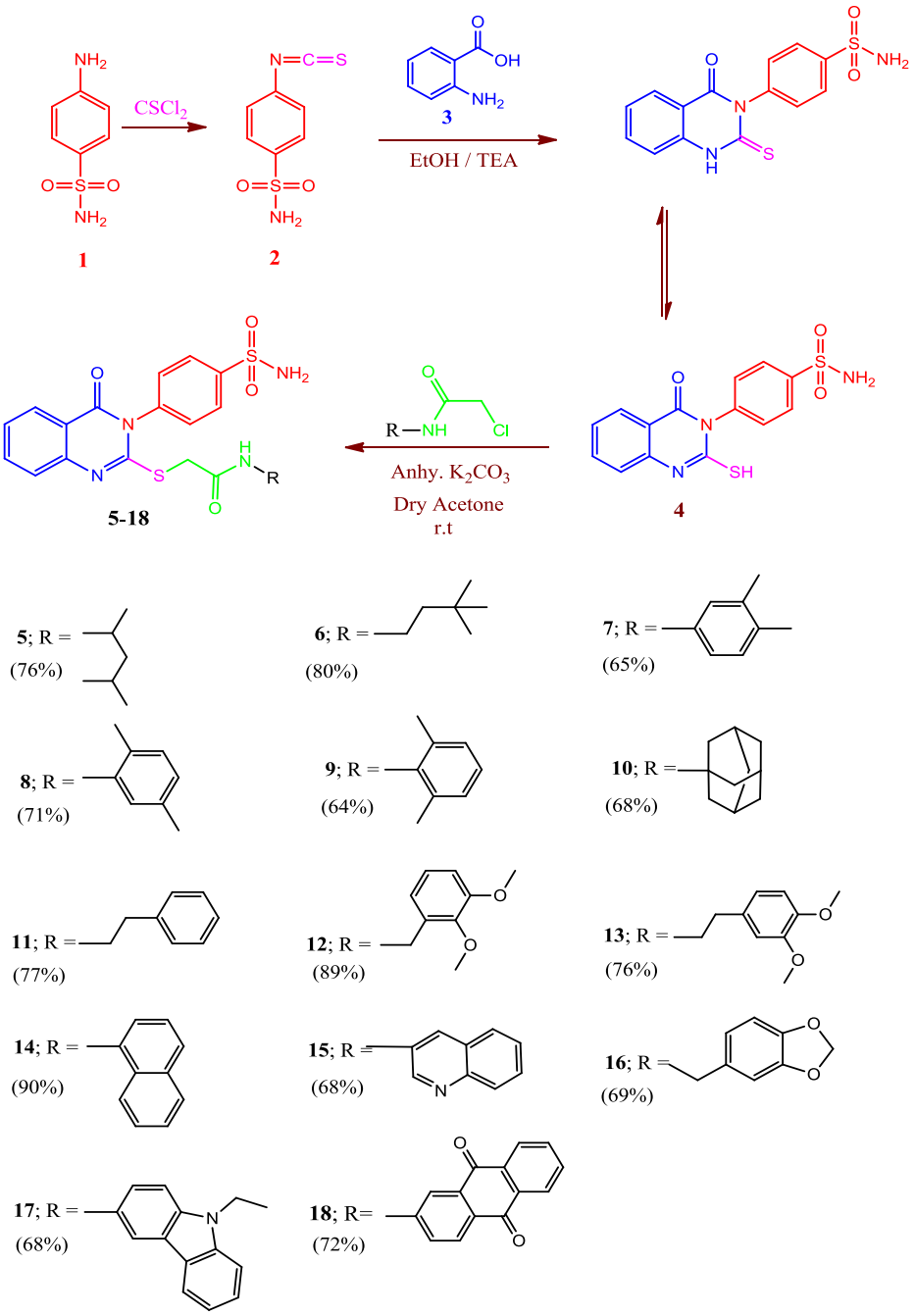


**Scheme 1.** Synthesis of the *N*-alkyl-2-[(4-oxo-3-(4-sulfamoylphenyl)-3,4-dihydroquinazolin-2-yl)thio]acetamide derivatives **5–18**. The yield of the reaction for each compound is expressed as (%) below it.

also measured. Molecular docking of the promising compound was performed inside the binding site of VEGFR-2 and EGFR to gain insights into the molecular interactions and possible mode of action.

## 2. Results and discussion

### 2.1. Chemistry

As depicted in scheme 1. The starting material 4-(2-mercapto-4-oxoquinazolin-3(4*H*)-yl) benzenesulfonamide **4** was first prepared from the reaction of sulfanilamide **1** with thiophosgene, followed by coupling of the anthranilic acid **3** with the formed 4-isothiocyanatobenzenesulfonamide **2** [29] to form the quinazolinone ring. When **4** reacted with 2-chloro-*N*-substituted acetamides in dry acetone and an equimolar amount of anhydrous $K_2CO_3$ at room temperature, a series of hybrid molecules **5–18** were formed by the introduction of different substitutions on the acetamide moiety to provide derivatives of varying lipophilic and electronic nature to study the structure-activity relationship (SAR). The structures of the target compounds **5–18** were confirmed by spectroscopic data. IR spectra of **5–18** are characterized by the presence of additional NH, $CH_2$ and CO bands at their specified ranges. $^1$H NMR spectra revealed singlet at the range of 3.80–4.31 ppm attributed to the S-$CH_2$, NH signal between 8.10 and 10.93 ppm, and the $SO_2NH_2$ singlet that lies in the aromatic region. $^{13}$C NMR spectra exhibited up-field signal for the S-$CH_2$ and two downfield signals for the 2CO carbons.

**Table 1**
Cytotoxicity and dual inhibitory activity of the target compounds against VEGFR-2 /EGFR.

| Sample code | $IC_{50}$ on MDA-MB-231 (μM)* | Residual concentration (pg/mL) | % inhibition of VEGFR-2 | $IC_{50}$ on VEGFR-2 (nM)* | $IC_{50}$ on EGFR (nM)* | $IC_{50}$ on MCF-10 (μM)* |
|---|---|---|---|---|---|---|
| **5** | 41.63 ± 1.31 | 1778 | 27.28 | – | – | – |
| **6** | 4.60 ± 0.11 | 516.4 | 78.87 | – | – | – |
| **7** | 9.31 ± 0.23 | 615.3 | 74.83 | – | – | – |
| **8** | 0.34 ± 0.01 | 253 | 89.65 | 487.20 ± 0.23 | 697.62 ± 0.40 | – |
| **9** | 4.31 ± 0.12 | 431.4 | 82.35 | – | – | – |
| **10** | 149.10 ± 3.47 | 1945 | 20.44 | – | – | – |
| **11** | 72.41 ± 1.24 | 1350 | 44.78 | – | – | – |
| **12** | 1.91 ± 0.04 | 426.5 | 82.55 | 247.38 ± 0.31 | 454.96 ± 0.20 | 37.00 ± 0.76 |
| **13** | 0.51 ± 0.01 | 278.8 | 88.59 | 731.95 ± 0.18 | 369.24 ± 0.16 | 97.15 ± 0.23 |
| **14** | 16.74 ± 0.39 | 739 | 69.77 | – | – | – |
| **15** | 141.66 ± 4.16 | 1837 | 24.86 | – | – | – |
| **16** | 2.61 ± 0.04 | 401.5 | 83.57 | 793.78 ± 0.33 | 470.73 ± 0.25 | – |
| **17** | 0.58 ± 0.01 | 242.2 | 90.09 | 693.65 ± 0.12 | 725.58 ± 0.27 | – |
| **18** | 5.42 ± 0.17 | 423.1 | 82.69 | – | – | – |
| **Erlotinib** | 0.73 ± 0.01 | – | – | – | 568.14 ± 0.61 | – |
| **Sunitinib** | 6.98 ± 0.52 | 766.9 | 67.73 | 320.20 ± 0.14 | – | – |

(–) Means not tested.
* The values represent the mean ± SE of three independent experiments.

### 2.2. Biological evaluation

#### 2.2.1. Measuring the cytotoxic activity against MDA-MB-231

To evaluate the anticancer activity of the new compounds, the cytotoxic activity of **5–18** was measured on MDA-MB-231 breast cancer cell line and compared to the reference drugs erlotinib & sunitinib. The results in Table 1 showed that the $IC_{50}$ of **5–18** was in the range of 0.34–149.10 μM. The 2,5-dimethyl derivative **8** was the most cytotoxic compound. The 3,4-dimethoxy phenethyl derivative **13** and the carbazole derivative **17** were more potent than the reference drug erlotinib ($IC_{50}$ = 0.51, 0.58 & 0.73 μM, respectively). The 2,3-dimethoxy benzyl derivative **12** and the piperonyl **16** also were active with $IC_{50}$ = 1.91 & 2.61 μM, respectively, and more cytotoxic than sunitinib ($IC_{50}$ = 6.98 μM). It is obvious from the results that the presence of methoxy groups as in **12** & **13** or heterocyclic rings containing oxygen or nitrogen in the terminal chain as in **16** & **17** improve the cytotoxic activity. The VEGFR-2 inhibition percentage of the compounds was measured and found in the range of 90.09–20.44 %. Compounds **8, 12, 13, 16** and **17** were the most active with inhibition percentage ranging from 90.09 to 82.55% compared to that of sunitinib (67.73%). These compounds were further chosen to measure the dual inhibitory activity on VEGFR-2 and EGFR.

#### 2.2.2. Dual VEGFR-2/EGFR inhibition

The promising compounds **8, 12, 13, 16** and **17** were screened on VEGFR-2 and EGFR enzymes in comparison to sunitinib & erlotinib. The $IC_{50}$ of these compounds against VEGFR-2 were in the range of 247–793 nM versus 369–725 nM for EGFR. Regarding the VEGFR-2 activity, the 2,3-dimethoxy benzyl derivative **12** was the most potent, followed by sunitinib and the 2,5-dimethyl phenyl derivative **8** ($IC_{50}$ 247, 320 and 487 nM, respectively). While for the EGFR, the 3,4-dimethoxy phenethyl derivative **13** was the most potent, followed by **12** and the piperonyl derivative **16** ($IC_{50}$ 369, 454 and 470 nM, respectively).

#### 2.2.3. Cytotoxicity on normal breast cell line

The poor selectivity of anticancer drugs is the major drawback in cancer treatment. In order to overcome this problem, the relative safety of compounds **12** & **13** was tested by measuring their cytotoxicity against MCF-10 normal breast cell line. Compounds **12** & **13** were found to possess moderate to low cytotoxicity on normal breast cells ($IC_{50}$ = 37 & 97 μM), and thus high selectivity to cancerous cells.

### 2.3. Radiosensitizing activity

Radiotherapy is considered the primary treatment for some types of cancers and sometimes received after chemotherapy or surgery. Radiotherapy using ionizing radiation can be used to shrink the tumor volume before the use of chemotherapy. Chemotherapy also can sensitize the tumor cells to the lethal effect of gamma (γ) irradiation. So, a combination of chemo-radiotherapy could be beneficial. In this research, the cytotoxicity of compounds **12** & **13** was screened against MDA-MB-231 cell line alone and when the cells containing the compounds were irradiated with a single dose of 8 Gy gamma radiation. From the results in Table 2, it is obvious that the $IC_{50}$ decreased after irradiation from $IC_{50}$ 1.91 & 0.51 to 0.79 & 0.43 μM for compounds **12** and **13**, respectively, and thus proving the radio-sensitizing activity of the tested compounds.

### 2.4. Molecular docking

Molecular docking was carried out to assess the mode of binding and interactions between the new compounds and the binding site inside the receptor compared to the co-crystallized ligand to rationalize the biological results. Most of the protein kinases share common features in their receptors. The ATP binding site consists of the hinge, ribose and the phosphate binding regions. Adjacent to these regions lies the hydrophobic region that may act as a target for some inhibitors [32]. The following PDB files were selected for this purpose; 4AGD for VEGFR-2 co-crystallized with sunitinib [33] and 1M17 for EGFR co-crystallized with erlotinib [34].

#### 2.4.1. Docking inside VEGFR-2 active site

The co-crystallized ligand sunitinib is located inside the hinge region of VEGFR-2 through its indol-2-one ring. Sunitinib binds through two hydrogen bonds, one binds the Glu 917 to the nitrogen of indolone and the

**Table 2**
$IC_{50}$ values of compounds **12** and **13** against MDA-MB-231 cells in combination with γ-radiation.

| Sample code | Control | Cells alone + 8 Gy $IC_{50}$ (μM)* | Cells + Compound + 8 Gy $IC_{50}$(μM)* |
|---|---|---|---|
| **12** | 1.000 | 0.98 ± 0.02 | 0.79 ± 0.13 |
| **13** | 1.000 | 0.98 ± 0.02 | 0.43 ± 0.21 |

Significant difference from the control group at $p < 0.001$.
* Each value is equivalent to the mean of three values ± Standard Error.

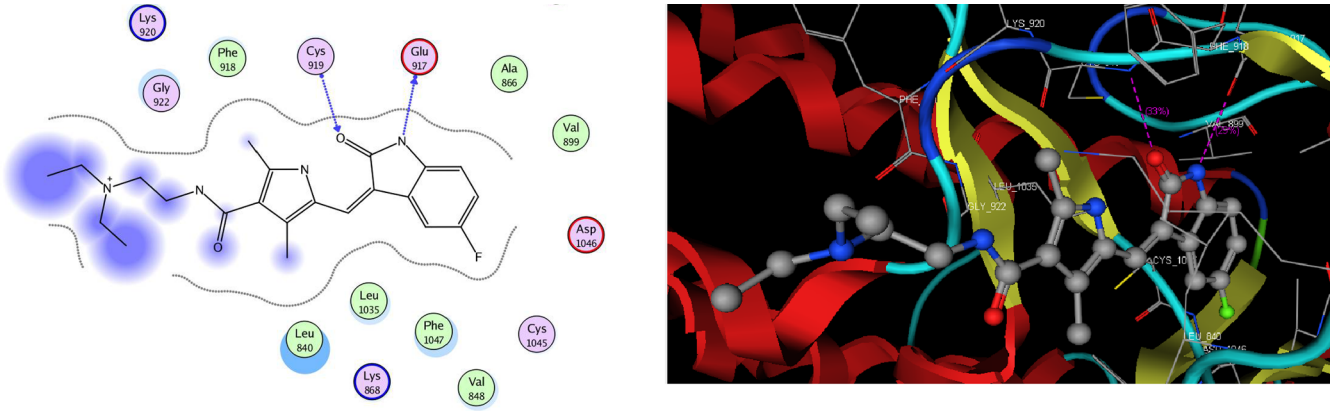


**Fig. 3.** Sunitinib is located inside the hinge region of **4AGD** by two hydrogen bonds, The Cys 919 binds to the carbonyl and Glu 917 binds to the N of the indolone.

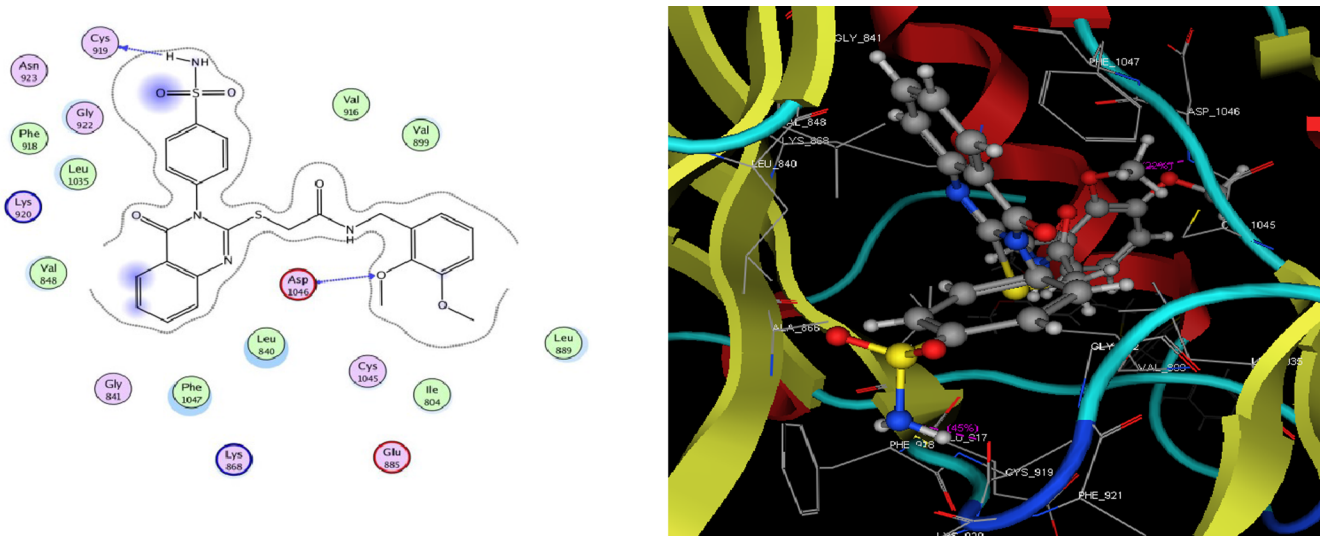


**Fig. 4.** Compound **12** forms two hydrogen bonds with **4AGD**. The NH of sulfonamide binds with Cys 919 and the methoxy with Asp 1046.

**Table 3**
Docking results of compound **12** inside the VEGFR-2 & EGFR active sites.

| Receptor | ligand | Energy score (S) (Kcal/mol) | Amino acids | Interacting groups | Length (Å) |
|---|---|---|---|---|---|
| **4AGD** | **Sunitinib** | −10.11 | Cys 919 | CO of indolone | 2.72 |
| | | | Glu 917 | N of indolone | 2.56 |
| | **12** | −12.01 | Cys 919 | NH of sulfonamide | 1.72 |
| | | | Asp 1046 | $OCH_3$ | 3.01 |
| **1 M17** | **Erlotinib** | −9.82 | Met 769 | N-1 of quinazoline | 2.70 |
| | **12** | −9.50 | Met 769 | NH of sulfonamide | 2.52 |
| | | | Pro 770 | | 2.84 |
| | | | Lys 721 | NH of sulfonamide Ph | 4.19 |

other binds Cys 919 to the carbonyl group [35]. For compound **12** the NH of sulfonamide and the methoxy group form two hydrogen bonds inside the binding pocket with Cys 919 and Asp 1046, respectively. The binding interactions of sunitinib and compound **12** in the active site of VEGFR-2 (PDB ID: 4AGD) were shown in Figs. 3 and 4, Table 3.

### 2.4.2. Docking inside EGFR active site

Quinazolines are hinge binder scaffolds for EGFR [36,37]. Erlotinib, the co-crystallized ligand, forms a hydrogen bond with Met 769 by its N-1 of the quinazoline moiety as reported in our previous work [27]. For compound **12**, the NH of sulfonamide makes two hydrogen bonds with Met 769 and Pro 770 along with the Lys 721 that forms a cation-pi interaction with the substituted phenyl ring. The binding interactions of compound **12** with EGFR (PDB ID: 1 M17) are shown in Fig. 5 and Table 3. Erlotinib and compound **12** can closely overlap in the binding pocket as represented in Fig. 6.

## 3. Conclusion

In summary, a hybridization strategy was adopted using the quinazolinone scaffold and sulfonamide moiety to produce the *N*-alkyl-2-[(4-oxo-3-(4-sulfamoylphenyl)-3,4-dihydroquinazolin-2-yl)thio]acetamide derivatives **5–18**. Different substitutions were introduced to the acetamide group to study the SAR. The cytotoxic activity of the synthesized compounds was screened against MDA-MB-231 breast cancer cells. The compounds showed $IC_{50}$ in the range of 0.34–149.10 μM. The 2,5-dimethyl derivative **8** was the most cytotoxic followed by the carbazole derivative **17** showing $IC_{50}$ 0.34 & 0.58 μM in reference to erlotinib & sunitinib $IC_{50}$ 0.73 & 6.98 μM, respectively. The percentage of inhibition towards VEGFR-2 varies in the range of 90.09 to 20.44% in reference to sunitinib (67.73%). The promising compounds **8, 12, 13, 16** and **17** were selected to measure the dual activity against VEGFR-2 and EGFR. The $IC_{50}$ of the promising compounds to VEGFR was in the range of 247–793 nM in reference to sunitinib ($IC_{50}$ 320 nM), while that of EGFR in the range of 369–725 nM in reference to erlotinib ($IC_{50}$

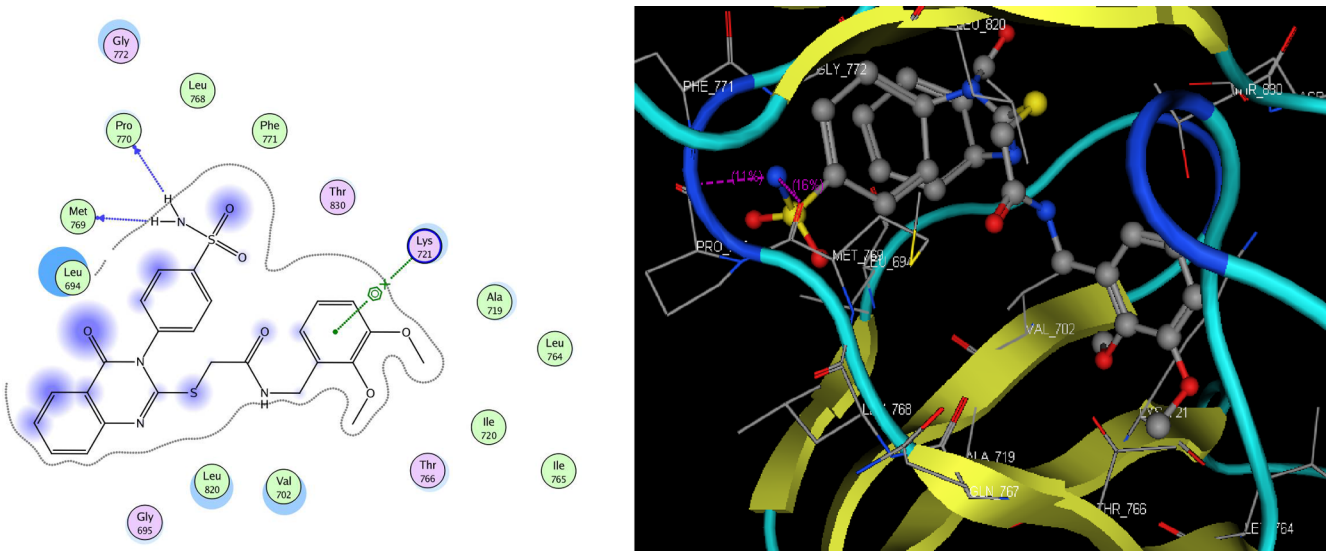


**Fig. 5.** 2D & 3D docking poses of compound **12** in the active site of **1M17**. The $NH_2$ of sulfonamide makes two hydrogen bonds with Met 769 and Pro770 along with the Lys 721 that forms a cation-π interaction with the substituted phenyl ring.

586 nM). Compound **12** was the most potent for VEGFR-2 and **13** for EGFR. The cytotoxicity against MCF-10 normal breast cell line was measured for **12** & **13** ($IC_{50}$ 37 & 97 μM, respectively) and proved their relative safety to normal breast cells. The radiosensitizing activity of **12** & **13** was studied on MDA-MB-231 cells after being irradiated by 8 Gy of gamma radiation. The compounds showed radiosensitizing activity with gamma radiation by relatively increasing cytotoxicity. Molecular docking of **12** in the binding sites of VEGFR-2 and EGFR confirmed the biological results. Finally, hybridization of quinazolinone with benzenesulfonamide has proved to be successful to provide potential multi-kinase inhibitors to act as anticancer and radiosensitizing agents.

## 4. Experimental

### 4.1. Chemistry

Melting points were measured uncorrected on a Gallen Kamp melting point apparatus (Sanyo Gallen Kamp, UK). A solvent system of chloroform/methanol (7:3) was used on a precoated silica gel plates (*Kieselgel* 0.25 mm, 60 F254, Merck, Germany) for TLC. IR spectra (KBr discs) were recorded using an FT-IR spectrophotometer (Perkin Elmer, USA). NMR spectra were scanned on an NMR spectrophotometer (Bruker AXS Inc., Switzerland), operating at 500 MHz for $^1H$ and 125.76 MHz for $^{13}C$. Chemical shifts were expressed in δ-values (ppm) relative to TMS as an internal standard, using DMSO-$d_6$ as a solvent. Mass spectra were recorded on the ISQ LT Thermo Scientific GCMS model (Massachusetts, USA). Elemental analyses were conducted on a model 2400 CHNSO analyzer (Perkin Elmer, USA). All the values are within ± 0.4% of the theoretical values. All reagents used were of AR grade.

#### 4.1.1. 4-(2-Mercapto-4-oxoquinazolin-3(4H)-yl) benzenesulfonamide (4)

A mixture of 4-isothiocyanatobenzenesulfonamide **2** (2.14 g, 0.01 mol) and anthranilic acid **3** (1.37 g, 0.01 mol) in absolute ethanol (30 mL) containing a catalytic amount of triethylamine, was refluxed for 2 h. The solid product formed was collected and crystallized from ethanol to give **4**.

Yield, 88%; m.p. 381.9 °C. IR: 3377, 3275 ($NH_2$), 3107 (arom.),

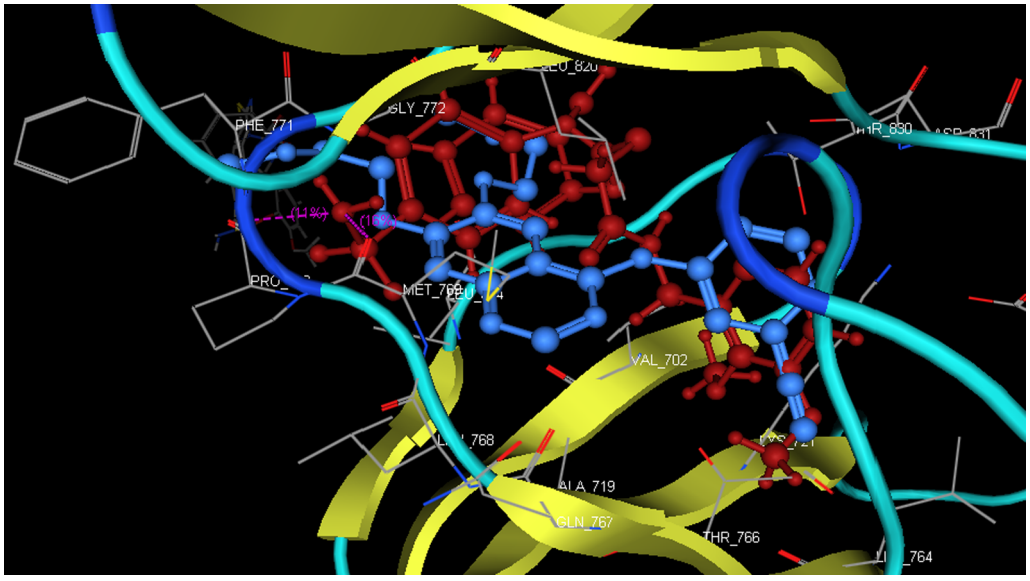


**Fig. 6.** Superimposition of compound **12** and erlotinib in the active site of **1M17**.

1710 (CO), 1624 (CN), 1340, 1159 ($SO_2$). $^1$HNMR (500 MHz, DMSO–$d_6$) δ: 2.1 (s, 1H), 7.46 (d, 2H, *J* = 7 Hz, AB), 7.79 (d, 1H, *J* = 10 Hz), 7.80–7.96 (m, 3H), 7.97 (d, 2H, *J* = 6 Hz, AB), 8.09 (s, 2H). $^{13}$CNMR (125 MHz, DMSO–$d_6$) δ: 116.2, 116.6 (2), 124.9, 127.0, 127.8, 130.3 (2), 136.2, 140.1, 142.6, 144.1, 160.2, 176.0. MS *m/z* (%): 333 ($M^+$) (12.52), 177 (1 0 0). Anal. Calcd. for $C_{14}H_{11}N_3O_3S_2$ (333.39): C, 50.44; H, 3.33; N, 12.60. Found: C, 50.67; H, 3.69; N, 12.88.

*4.1.2. N-alkyl-2-[(4-oxo-3-(4-sulfamoylphenyl)-3,4-dihydroquinazolin-2-yl)thio]acetamide derivatives **5–18***

General procedure

A mixture of **4** (3.33 g, 0.01 mol) and 2-chloro-*N*-substituted acetamide derivatives (0.012 mol) in dry acetone (50 mL) and anhydrous $K_2CO_3$ (1.38 g, 0.01 mol) was stirred at room temperature for 12 h, filtered and the solid product formed was crystallized from ethanol to give **5–18.**

*4.1.2.1. N-(4-Methylpentan-2-yl)-2-[(4-oxo-3-(4-sulfamoylphenyl)-3,4-dihydroquinazolin-2-yl)thio]acetamide **(5)***. **5:** Yield, 76%; m.p. 205.3 °C. IR: 3414, 3334, 3229 ($NH_2$, NH), 3080 (arom.), 2958, 2867 (aliph.), 1703, 1654 (2CO), 1544 (CN), 1340, 1163 ($SO_2$). $^1$HNMR (500 MHz, DMSO–$d_6$) δ: 0.79 (d, 6H, *J* = 4 Hz), 1.15 (d, 3H, *J* = 4.5 Hz), 1.32 (t, 2H, *J* = 8.5 Hz), 1.54–1.57 (m, 1H), 3.80 (s, 2H), 3.87–3.90 (m, 1H), 7.49 (d, 2H, *J* = 10 Hz, AB), 7.58 (d, 1H, *J* = 10 Hz), 7.86–8.03 (m, 3H), 8.04 (d, 2H, *J* = 8 Hz, AB), 8.09 (s, 2H), 8.10 (d, 1H, *J* = 4 Hz). $^{13}$CNMR (125 MHz, DMSO–$d_6$) δ: 21.7, 22.5 (2), 23.2, 24.8, 43.2, 45.8, 119.9 (2), 123.4, 126.4, 126.6, 127.0, 127.4 (2), 130.7, 135.5, 138.9, 146.2, 156.7, 161.0, 165.8. MS *m/z* (%): 474 ($M^+$) (1.21), 374 (1 0 0). Anal. Calcd. for $C_{22}H_{26}N_4O_4S_2$ (474.60): C, 55.68; H, 5.52; N, 11.81. Found: C, 55.32; H, 5.28; N, 11.49.

*4.1.2.2. N-(3,3-Dimethylbutyl)-2-[(4-oxo-3-(4-sulfamoylphenyl)-3,4-dihydroquinazolin-2-yl)thio]acetamide **(6)***. **6:** Yield, 80%; m.p. 267.9 °C. IR: 3434, 3390, 3212 ($NH_2$, NH), 3100 (arom.), 2956, 2833 (aliph.), 1701, 1654 (2CO), 1568 (CN), 1338, 1163 ($SO_2$). $^1$HNMR (500 MHz, DMSO–$d_6$) δ: 0.86 (s, 9H), 1.32 (t, 2H, *J* = 10 Hz), 3.05 (m, 2H), 3.87 (s, 2H), 7.49 (d, 2H, *J* = 5.5 Hz, AB), 7.67–7.99 (m, 4H), 8.00 (d, 2H, *J* = 10 Hz, AB), 8.08 (s, 2H), 8.10 (t, 1H, *J* = 6.5 Hz). $^{13}$CNMR (125 MHz, DMSO–$d_6$) δ: 29.6, 30.0 (4), 36.8, 43.1, 119.9 (3), 126.5, 126.6 (2), 127.0, 127.3, 130.5, 135.5, 138.5, 147.6, 156.7, 161.1, 166.5. MS *m/z* (%): 475 ($M^+ + 1$) (17.48), 474 ($M^+$) (1 0 0). Anal. Calcd. for $C_{22}H_{26}N_4O_4S_2$ (474.60): C, 55.68; H, 5.52; N, 11.81. Found: C, 55.98; H, 5.87; N, 12.12.

*4.1.2.3. N-(3,4-Dimethylphenyl)-2-[(4-oxo-3-(4-sulfamoylphenyl)-3,4-dihydroquinazolin-2-yl)thio]acetamide **(7)***. **7:** Yield, 65%; m.p. 244.4 °C. IR: 3409, 3365, 3290 ($NH_2$, NH), 3064 (arom.), 2920, 2857 (aliph.), 1681, 1660 (2CO), 1610 (CN), 1336, 1163 ($SO_2$). $^1$HNMR (500 MHz, DMSO–$d_6$) δ: 2.17 (s, 6H), 4.11 (s, 2H), 7.30 (s, 1H), 7.31–7.48 (m, 2H), 7.49 (d, 2H, *J* = 10 Hz, AB), 7.83 (d, 1H, *J* = 6 Hz), 7.86–8.03 (m, 3H), 8.04 (d, 2H, *J* = 8 Hz, AB), 8.08 (s, 2H), 10.3 (s, 1H). $^{13}$CNMR (125 MHz, DMSO–$d_6$) δ: 19.2, 20.1, 37.8, 117.1, 119.9, 120.8 (2), 126.4, 126.6 (2), 127.0, 127.4, 130.0 (2), 130.7, 131.6, 135.5 (2), 136.8, 137.1, 147.5, 156.6, 161.0, 165.6. MS *m/z* (%): 496 ($M^+ + 2$) (3.86), 495 ($M^+ + 1$) (35.10), 494 ($M^+$) (1 0 0). Anal. Calcd. for $C_{24}H_{22}N_4O_4S_2$ (494.59): C, 58.28; H, 4.48; N, 11.33. Found: C, 58.50; H, 4.75; N, 11.70.

*4.1.2.4. N-(2,5-Dimethylphenyl)-2-[(4-oxo-3-(4-sulfamoylphenyl)-3,4-dihydroquinazolin-2-yl)thio]acetamide **(8)***. **8:** Yield, 71%; m.p. 262.8 °C. IR: 3325, 3273, 3234 ($NH_2$, NH), 3088 (arom.), 2978, 2918 (aliph.), 1688, 1656 (2CO), 1546 (CN), 1332, 1163 ($SO_2$). $^1$HNMR (500 MHz, DMSO–$d_6$) δ: 2.15, 2.21 (2 s, 6H), 4.15 (s, 2H), 6.89 (d, 1H, *J* = 5 Hz), 7.07 (d, 1H, *J* = 5 Hz), 7.19 (s, 1H), 7.49 (d, 2H, *J* = 10 Hz, AB), 7.86 (d, 1H, *J* = 5.5 Hz), 7.50–7.64 (m, 3H), 8.09 (d, 2H, *J* = 5 Hz, AB), 7.99 (s, 2H), 9.80 (s, 1H). $^{13}$CNMR (125 MHz, DMSO–$d_6$) δ: 17.9, 21.0, 37.0, 119.9 (2), 125.9 (2), 126.5, 126.6, 127.1, 127.2, 129.1, 130.2, 130.5 (2), 135.4, 135.5 (2), 136.3 (2), 147.6, 158.7, 161.1, 166.0. MS *m/z* (%): 494 ($M^+$) (8.09), 460 (1 0 0). Anal. Calcd. for $C_{24}H_{22}N_4O_4S_2$ (494.59): C, 58.28; H, 4.48; N, 11.33. Found: C, 58.63; H, 4.82; N, 11.65.

*4.1.2.5. N-(2,6-Dimethylphenyl)-2-[(4-oxo-3-(4-sulfamoylphenyl)-3,4-dihydroquinazolin-2-yl)thio]acetamide **(9)***. **9:** Yield, 64%; m.p. 258.2 °C. IR: 3392, 3300, 3215 ($NH_2$, NH), 3074 (arom.), 2920, 2832 (aliph.), 1680, 1654 (2CO), 1608 (CN), 1340, 1163 ($SO_2$). $^1$HNMR (500 MHz, DMSO–$d_6$) δ: 2.12 (s, 6H), 4.17 (s, 2H), 7.05–7.06 (m, 3H), 7.50 (d, 2H, *J* = 5 Hz, AB), 7.70 (d, 1H, *J* = 5.5 Hz), 7.87–78.01 (m, 3H), 8.11 (d, 2H, *J* = 5 Hz, AB), 8.01 (s, 2H), 9.8 (s, 1H). $^{13}$CNMR (125 MHz, DMSO–$d_6$) δ: 18.5 (2), 31.7, 119.9 (3), 126.5, 126.6, 127.0, 127.1, 127.3 (2), 128.0 (2), 130.5 (2), 135.5, 135.7, 138.4 (2), 147.3, 156.6, 161.1, 165.6. MS *m/z* (%): 495 ($M^+ + 1$) (30.81), 494 ($M^+$) (35.14), 407 (1 0 0). Anal. Calcd. for $C_{24}H_{22}N_4O_4S_2$ (494.59): C, 58.28; H, 4.48; N, 11.33. Found: C, 58.49; H, 4.61; N, 11.59.

*4.1.2.6. N-(adamantan-1-yl)-2-[(4-oxo-3-(4-sulfamoylphenyl)-3,4-dihydroquinazolin-2-yl)thio]acetamide **(10)***. **10:** Yield, 68%; m.p. 88.3 °C. IR: 3348, 3300, 3251 ($NH_2$, NH), 3066 (arom.), 2906,2850 (aliph.), 1678, 1658 (2CO), 1612 (CN), 1336, 1161 ($SO_2$). $^1$HNMR (500 MHz, DMSO–$d_6$) δ: 1.60–1.62 (m, 6H), 1.91–1.98 (m, 3H), 2.01 (d, 6H, *J* = *10* Hz), 3.96 (s, 2H), 7.50 (d, 2H, *J* = 5.2 Hz, AB), 7.82 (d, 1H, *J* = 5 Hz), 7.87–8.03 (m, 3H), 8.04 (d, 2H, *J* = 6 Hz, AB), 8.09 (s, 2H), 8.10 (s, 1H). $^{13}$CNMR (125 MHz, DMSO–$d_6$) δ: 29.2, 31.1 (3), 36.3 (3), 43.3 (3), 51.6, 119.9, 126.4 (2), 126.5, 127.0, 127.4, 130.8 (2), 135.5 (2), 139.1, 147.6, 161.0, 165.2, 165.8. MS *m/z* (%): 526 ($M^+ + 2$) (3.29), 525 ($M^+ + 1$) (6.23), 524 ($M^+$) (20.33), 94 (1 0 0). Anal. Calcd. for $C_{26}H_{28}N_4O_4S_2$ (524.65): C, 59.52; H, 5.38; N, 10.68. Found: C, 59.20; H, 5.02; N, 10.34.

*4.1.2.7. 2-[(4-Oxo-3-(4-sulfamoylphenyl)-3,4-dihydroquinazolin-2-yl) thio]-N-phenethyl acetamide **(11)***. **11:** Yield, 77%; m.p. 220.5 °C. IR: 3325, 3273, 3152 ($NH_2$, NH), 3093 (arom.), 2953, 2883 (aliph.), 1680, 1647 (2CO), 1550 (CN), 1379, 1159 ($SO_2$). $^1$HNMR (500 MHz, DMSO–$d_6$) δ: 2.71 (t, 2H, *J* = 5 Hz), 3.30 (m, 2H), 3.89 (s, 2H), 7.17 (d, 1H, *J* = 6 Hz), 7.18 (d, 1H, *J* = 5 Hz), 7.25–7.50 (m, 3H), 7.51 (d, 2H, *J* = 6 Hz, AB), 7.71–7.86 (m, 4H), 8.03 (d, 2H, *J* = 5.5 Hz, AB), 8.09 (s, 2H), 8.30 (t, 1H, *J* = 7 Hz). $^{13}$CNMR (125 MHz, DMSO–$d_6$) δ: 35.4, 36.6, 39.5, 119.9 (3), 126.5, 126.6, 127.0, 127.4, 128.7 (2), 129.0 (2), 130.8 (2), 135.5, 139.0, 139.6, 145.8, 147.5, 156.5, 161.1, 166.9. MS *m/z* (%): 496 ($M^+ + 2$) (5.50), 495 ($M^+ + 1$) (17.10), 494 ($M^+$) (59.70), 63 (1 0 0). Anal. Calcd. for $C_{24}H_{22}N_4O_4S_2$ (494.59): C, 58.28; H, 4.48; N, 11.33. Found: C, 58.50; H, 4.89; N, 11.59.

*4.1.2.8. N-(2,3-Dimethoxybenzyl)-2-[(4-oxo-3-(4-sulfamoylphenyl)-3,4-dihydroquinazolin-2-yl)thio]acetamide **(12)***. **12:** Yield, 89%; m.p. 244.6 °C. IR: 3408, 3323, 3280 ($NH_2$, NH), 3077 (arom.), 2953, 2912 (aliph.), 1688, 1646 (2CO), 1608 (CN), 1398, 1163 ($SO_2$). $^1$HNMR (500 MHz, DMSO–$d_6$) δ: 3.71, 3.78 (2 s, 6H), 3.98 (s, 2H), 4.29 (d, 2H, *J* = 4.5 Hz), 6.84 (d, 1H, *J* = 7 Hz), 6.92 (m, 2H), 7.51 (d, 2H, *J* = 6 Hz, AB), 7.57 (d, 1H, *J* = 6.5 Hz), 7.61–7.87 (m, 3H), 8.03 (s, 2H), 8.04 (d, 2H, *J* = 6 Hz, AB), 8.58 (t, 1H, *J* = 4.5 Hz). $^{13}$CNMR (125 MHz, DMSO–$d_6$) δ: 36.5, 37.9, 56.1, 60.4, 112.1, 119.9, 120.4, 124.1 (3), 126.6, 126.7, 127.0, 127.4, 130.8 (2), 132.6, 135.5, 139.1, 145.8, 146.5, 147.5, 156.5, 161.1, 167.0. MS *m/z* (%): 540 ($M^+$) (21.72), 509 (1 0 0). Anal. Calcd. for $C_{25}H_{24}N_4O_6S_2$ (540.61): C, 55.54; H, 4.47; N, 10.36. Found: C, 55.31; H, 4.24; N, 10.08.

*4.1.2.9. N-(3,4-Dimethoxyphenethyl)-2-[(4-oxo-3-(4-sulfamoylphenyl)-3,4-dihydroquinazolin-2-yl)thio]acetamide **(13)***. **13:** Yield, 76%; m.p. 254.7 °C. IR: 3371, 3300, 3230 ($NH_2$, NH), 3100 (arom.), 2922, 2839

(aliph.), 1670, 1654 (2CO), 1610 (CN), 1371, 1159 ($SO_2$). $^1$HNMR (500 MHz, DMSO–$d_6$) δ: 2.64 (t, 2H, *J* = 5 Hz), 3.30 (m, 2H), 3.70, 3.71 (2 s, 6H), 3.90 (s, 2H), 6.65–6.79 (m, 3H), 7.49 (d, 2H, *J* = 5 Hz, AB), 7.71 (d, 1H, *J* = 6.5 Hz), 7.84–7.86 (m, 3H), 8.03 (s, 2H), 8.04 (d, 2H, *J* = 5 Hz, AB), 8.26 (t, 1H, *J* = 4.5 Hz). $^{13}$CNMR (125 MHz, DMSO–$d_6$) δ: 31.1, 34.9, 36.6, 55.8 (2), 112.1, 112.7, 119.9, 120.8 (2), 126.5, 126.6, 127.0, 127.4, 130.8 (2), 132.0, 135.5, 139.0, 145.8, 147.5, 147.6, 149.6, 156.4, 161.1. 166.9. MS *m/z* (%): 554 ($M^+$) (3.14), 432 (1 0 0). Anal. Calcd. for $C_{26}H_{26}N_4O_6S_2$ (554.64): C, 56.30; H, 4.72; N, 10.10. Found: C, 56.59; H, 5.01; N, 10.36.

*4.1.2.10. N-(Naphthalen-1-yl)-2-[(4-oxo-3-(4-sulfamoylphenyl)-3,4-dihydroquinazolin-2-yl)thio]acetamide (**14**).* **14:** Yield, 90%; m.p. 257.8 °C. IR: 3385, 3321, 3256 ($NH_2$, NH), 3100 (arom.), 2963, 2824 (aliph.), 1674, 1654 (2CO), 1606 (CN), 1398, 1159 ($SO_2$). $^1$HNMR (500 MHz, DMSO–$d_6$) δ: 4.31 (s, 2H), 7.49 (d, 2H, *J* = 6 Hz, AB), 7.51–7.62 (m, 6H), 7.72–7.75 (m, 3H), 7.77 (d, 1H, *J* = 6 Hz), 7.78 (s, 2H), 8.04 (d, 2H, *J* = 5 Hz, AB), 8.15 (d, 1H, *J* = 5 Hz), 10.30 (s, 1H). $^{13}$CNMR (125 MHz, DMSO–$d_6$) δ: 31.8, 120.0 (2), 122.4, 123.4, 126.0 (2), 126.1, 126.2, 126.5, 126.6, 126.7, 127.1, 127.4, 128.4, 128.5 (2), 130.8, 133.8, 134.1, 135.6, 139.1, 146.0, 156.7, 161.1, 166.8. MS *m/z* (%): 516 ($M^+$) (32.04), 319 (1 0 0). Anal. Calcd. for $C_{26}H_{20}N_4O_4S_2$ (516.59): C, 60.45; H, 3.90; N, 10.85. Found: C, 60.16; H, 3.59; N, 10.64.

*4.1.2.11. 2-(4-Oxo-3-[(4-sulfamoylphenyl)-3,4-dihydroquinazolin-2-yl) thio]-N-(quinolin-3-yl)acetamide (**15**).* **15:** Yield, 68%; m.p. 312.7 °C. IR: 3415, 3304, 3251 ($NH_2$, NH), 3100 (arom.), 2971, 2881 (aliph.), 1693, 1656 (2CO), 1635 (CN), 1396, 1186 ($SO_2$). $^1$HNMR (500 MHz, DMSO–$d_6$) δ: 4.23 (s, 2H), 7.48 (s, 1H), 7.57 (d, 2H, *J* = 7 Hz, AB), 7.58–7.79 (m, 4H), 7.80–7.91 (m, 4H), 7.95 (d, 2H, *J* = 8 Hz, AB), 8.69 (s, 1H), 8.98 (s, 2H) 10.93 (s, 1H). $^{13}$CNMR (125 MHz, DMSO–$d_6$) δ: 37.6, 122.6 (3), 126.4 (2), 126.7 (2), 127.1, 127.5 (2), 127.6, 128.1, 128.4, 129.0, 130.8, 133.1, 144.7 (2), 144.8, 145.9, 147.5, 156.4, 161.0, 167.1. MS *m/z* (%): 517 ($M^+$) (11.53), 170 (1 0 0). Anal. Calcd. for $C_{25}H_{19}N_5O_4S_2$ (517.58): C, 58.01; H, 3.70; N, 13.53. Found: C, 58.32; H, 3.94; N, 13.87.

*4.1.2.12. N-(Benzo[d][1,3]dioxol-5-ylmethyl)-2-(4-oxo-3-(4-sulfamoylphenyl)-3,4-dihydroquinazolin-2-ylthio) acetamide (**16**).* **16:** Yield, 69%; m.p. 254.7 °C. IR: 3317, 3253, 3166 ($NH_2$, NH), 3066 (arom.), 2985, 2924 (aliph.), 1691, 1643 (2CO), 1621 (CN), 1398, 1157 ($SO_2$). $^1$HNMR (500 MHz, DMSO–$d_6$) δ: 3.96 (s, 2H), 4.20 (d, 2H, *J* = 6 Hz), 5.96 (s, 2H), 6.74–6.82 (m, 3H), 7.51 (d, 2H, *J* = 7 Hz, AB), 7.52–7.84 (m, 4H), 8.03 (d, 2H, *J* = 7 Hz, AB), 8.05 (s, 2H), 8.65 (t, 1H, *J* = 4.5 Hz). $^{13}$CNMR (125 MHz, DMSO–$d_6$) δ: 36.5, 42.7, 101.2, 108.3, 108.4, 119.9, 120.8 (3), 126.6, 127.0, 127.4, 130.8 (2), 133.4 (2), 135.4, 139.1, 145.4, 146.5, 147.5, 156.4, 161.1, 166.9. MS *m/z* (%): 525 ($M^+ + 1$) (5.92), 524 ($M^+$) (21.05), 98 (1 0 0). Anal. Calcd. for $C_{24}H_{20}N_4O_6S_2$ (524.57): C, 54.95; H, 3.84; N, 10.68. Found: C, 54.59; H, 3.48; N, 10.32.

*4.1.2.13. N-(9-Ethyl-9H-carbazol-3-yl)-2-(4-oxo-3-(4-sulfamoylphenyl)-3,4-dihydroquinazolin-2-ylthio) acetamide (**17**).* **17:** Yield, 68%; m.p. 276.4 °C. IR: 3392, 3273, 3143 ($NH_2$, NH), 3064 (arom.), 2913, 2873 (aliph.), 1681, 1654 (2CO), 1610 (CN), 1336, 1181 ($SO_2$). $^1$HNMR (500 MHz, DMSO–$d_6$) δ: 1.28 (t, 3H, *J* = 5 Hz), 4.19 (s, 2H), 4.42 (q, 2H, *J* = 4 Hz), 7.16–7.45 (m, 7H), 7.49 (d, 2H, *J* = 5 Hz, AB), 7.64 (d, 1H, *J* = 7 Hz), 7.70–8.02 (m, 3H), 8.03 (d, 2H, *J* = 8 Hz, AB), 8.43 (s, 2H), 10.40 (s, 1H). $^{13}$CNMR (125 MHz, DMSO–$d_6$) δ: 14.1, 39.8, 40.0, 109.5, 109.6, 111.7 (2), 119.0, 119.3, 119.9, 120.6, 122.3, 122.4 (2), 126.2, 126.5, 126.6, 127.1, 127.3, 130.5, 131.3 (2), 135.5 (2), 136.7, 138.4, 147.6, 156.8, 161.1, 165.5. MS *m/z* (%): 584 ($M^+ + 1$) (18.43), 583 ($M^+$) (39.02), 134 (1 0 0). Anal. Calcd. for $C_{30}H_{25}N_5O_4S_2$ (583.68): C, 61.73; H, 4.32; N, 12.00. Found: C, 61.96; H, 4.61; N, 12.28.

*4.1.2.14. N-(9,10-Dioxo-9,10-dihydroanthracen-2-yl)-2-(4-oxo-3-(4-sulfamoylphenyl)-3,4-dihydroquinazolin-2-ylthio) acetamide (**18**).* **18:** Yield, 72%; m.p. 287.4 °C. IR: 3367, 3261, 3200 ($NH_2$, NH), 3057 (arom.), 2953, 2819 (aliph.), 1703, 1695, 1680, 1654 (4CO), 1587 (CN), 1398, 1163 ($SO_2$). $^1$HNMR (500 MHz, DMSO–$d_6$) δ: 4.20 (s, 2H), 7.52 (d, 2H, *J* = 6 Hz, AB), 7.53–7.79 (m, 4H), 7.80–8.06 (m, 7H), 8.09 (d, 2H, *J* = 5 Hz, AB), 8.18 (s, 2H), 8.50 (s, 1H). $^{13}$CNMR (125 MHz, DMSO–$d_6$) δ: 31.1, 116.2, 119.9, 124.2 (2), 126.4, 126.6, 127.0, 127.1 (2), 127.2, 127.5, 128.5, 129.0 (2), 130.8 (2), 133.5, 134.6 (2), 134.7, 135.0, 139.0, 144.8, 145.9, 156.4, 161.0, 167.2, 182.8 (2). MS *m/z* (%): 596 ($M^+$) (1.67), 315 (1 0 0). Anal. Calcd. for $C_{30}H_{20}N_4O_6S_2$ (596.63): C, 60.39; H, 3.38; N, 9.39. Found: C, 60.08; H, 3.06; N, 9.12.

### 4.2. Biological evaluation

#### 4.2.1. MTT assay

The cytotoxic activity screening was performed on MDA-MB-231 and MCF-10 breast cancer and normal cells, obtained from American Type Culture Collection. Cells were cultured using DMEM (Dulbecco's Modified Eagle's Medium) supplemented with 10% fetal bovine serum, 10 μg/mL of insulin, and 1% penicillin-streptomycin at 37 °C in a humidified atmosphere containing 5% CO2. Cells were seeded in 96-well plate with cells density 1.2–1.8 × 10,000 cells/well, in a volume of 100 μL complete growth medium with 100 μL of the tested compound per well and the plate was incubated for 24 h before the MTT assay. Then, rinse the cell layer with 0.25% (w/v) Trypsin, 0.53 mM EDTA solution. 1 mg/mL of each tested compound was added to the media and incubated for 2–4 h. Color intensity was measured using an enzyme-linked immunosorbent assay ELISA reader at wavelength of 570 nm. $IC_{50}$ was calculated from the survival curve using Graph Pad Prism 5 and compared to the reference drugs erlotinib and sunitinib.

#### 4.2.2. In vitro VEGFR-2 and EGFR enzymatic assay

EGFR kinase kit (PV3872) 0.200 mg/mL and VEGFR-2 anti-phosphotyrosine antibody with the alpha screen system (PerkinElmer, USA) were used for enzymatic activity screening according to the manufacturer's instructions as previously reported [27,29]. The inhibition percentage of VEGFR-2 was calculated by comparing the activity of the tested compounds to control.

### 4.3. Radiosensitizing activity

Irradiation was performed at the National Center for Radiation Research and Technology (NCRRT), Egyptian Atomic Energy Authority (EAEA), using Gamma cell-40 ($^{137}$Cs) source. The most potent compounds in the VEGFR-2 and EGFR assay **12** & **13** were selected to measure the cytotoxic activity in combination with gamma irradiation. The MDA-MB-231 Cells were plated in 96-multiwell plate and incubated at 37 °C in an atmosphere of 5% $CO_2$ for 48 h before irradiation. In another plate, cells were incubated for 2 h with compounds **12** & **13** in molar concentrations of 0.01, 0.1, 1.0 and 10 μM. Cells were irradiated by a single dose of γ- radiation at a dose level of 8 Gy with a dose rate of 0.758 rad/*sec* for 17.73 min, and then cytotoxicity was measured 48 h after irradiation. Color intensity was measured by an ELISA reader at 570 nm. The surviving fractions were expressed as mean values ± standard error. The results were analyzed using a 1-way ANOVA test.

### 4.4. Molecular docking

The molecular modeling studies were fulfilled by the Molecular Operating Environment software (MOE, 10.2008). Energy minimizations were performed with an RMSD gradient of 0.01 kcal $mol^{-1}$ $Å^{-1}$with MMFF94X force field and the partial charges were automatically calculated. Two receptors were chosen from the protein data bank; 4AGD that represents VEGFR-2 co-crystallized with

sunitinib and 1M17 for EGFR co-crystallized with erlotinib. Both enzymes were prepared for docking by ignoring water in the receptor. Hydrogen atoms were added to the structure with their standard geometry. The co-crystallized ligands in both receptors were used to determine the binding site. Validation of the procedure was performed by re-docking of the co-crystallized ligands into the active sites of VEGFR-2 & EGFR enzymes followed by docking of compound **12**. Docking poses with an energy score (S) = $-9.82$ and $-10.11\ \text{kcal mol}^{-1}$ were obtained for erlotinib and sunitinib, respectively. The obtained data were used to interpret the ligand-enzyme interactions at the active site.

## Acknowledgement

The authors appreciate the staff members of the gamma irradiation unit at the National Center for Radiation Research and Technology (NCRRT) for carrying out the irradiation process.

## References

[1] C. Peitzsch, R. Perrin, R.P. Hill, A. Dubrovska, I. Kurth, Hypoxia as a biomarker for radioresistant cancer stem cells, Int. J. Radiat. Biol. 90 (2014) 636–652.
[2] F. Broekman, E. Giovannetti, G.J. Peters, Tyrosine kinase inhibitors: Multi-targeted or single-targeted? World J. Clin. Oncol. 2 (2011) 80–93.
[3] T. Sugrue, N.F. Lowndes, R. Ceredig, Hypoxia enhances the radioresistance of mouse mesenchymal stromal cells, Stem Cells 32 (2014) 2188–2200.
[4] C. Wang, H. Wu, V. Katritch, G.W. Han, X.-P. Huang, W. Liu, F.Y. Siu, B.L. Roth, V. Cherezov, R.C. Stevens, Structure of the human smoothened receptor bound to an antitumour agent, Nature 497 (2013) 338–343.
[5] S. Blagden, J.d. Bono, Drugging cell cycle kinases in cancer therapy, Curr. Drug Targets 6 (2005) 325–335.
[6] L. Kondapalli, K. Soltani, M.E. Lacouture, The promise of molecular targeted therapies: protein kinase inhibitors in the treatment of cutaneous malignancies, J. Am. Acad. Dermatol. 53 (2005) 291–302.
[7] P. Cohen, Protein kinases—the major drug targets of the twenty-first century? Nat. Rev. Drug Discov. 1 (2002) 309–315.
[8] D.R. Knighton, J. Zheng, L.F. Ten Eyck, V.A. Ashford, N.H. Xuong, S.S. Taylor, J.M. Sowadski, Crystal structure of the catalytic subunit of cyclic adenosine monophosphate-dependent protein kinase, Science 253 (1991) 407–414.
[9] A. Arora, E.M. Scholar, Role of tyrosine kinase inhibitors in cancer therapy, J. Pharmacol. Exp. Ther. 315 (2005) 971–979.
[10] I. Shchemelinin, L. Sefc, E. Necas, Protein kinases, their function and implication in cancer and other diseases, Folia Biol. 52 (2006) 81–100.
[11] S. Grant, Therapeutic protein kinase inhibitors, Cell. Mol. Life Sci. 66 (2009) 1163–1177.
[12] B. Zahorowska, P.J. Crowe, J.L. Yang, Combined therapies for cancer: a review of EGFR-targeted monotherapy and combination treatment with other drugs, J. Cancer Res. Clin. Oncol. 135 (2009) 1137–1148.
[13] L. Garuti, M. Roberti, G. Bottegoni, Multi-kinase inhibitors, Curr. Med. Chem. 22 (2015) 695–712.
[14] S.R. Hubbard, J.H. Till, Protein tyrosine kinase structure and function, Annu. Rev. Biochem. 69 (2000) 373–398.
[15] D.R. Senger, S.J. Galli, A.M. Dvorak, C.A. Perruzzi, V.S. Harvey, H.F. Dvorak, Tumor cells secrete a vascular permeability factor that promotes accumulation of ascites fluid, Science 219 (1983) 983–985.
[16] P. Carmeliet, R.K. Jain, Molecular mechanisms and clinical applications of angiogenesis, Nature 473 (2011) 298–307.
[17] C. Yewale, D. Baradia, I. Vhora, S. Patil, A. Misra, Epidermal growth factor receptor targeting in cancer: a review of trends and strategies, Biomaterials 34 (2013) 8690–8707.
[18] E. Zwick, J. Bange, A. Ullrich, Receptor tyrosine kinase signalling as a target for cancer intervention strategies, Endocr. Relat. Cancer 8 (2001) 161–173.
[19] R.S. Herbst, Review of epidermal growth factor receptor biology, Int. J. Radiat. Oncol. Biol. Phys. 59 (2004) S21–S26.
[20] L.V. Sequist, T.J. Lynch, EGFR tyrosine kinase inhibitors in lung cancer: an evolving story, Annu. Rev. Med. 59 (2008) 429–442.
[21] D. Pytel, T. Sliwinski, T. Poplawski, D. Ferriola, I. Majsterek, Tyrosine kinase blockers: new hope for successful cancer therapy, Anti-Cancer Agents Med. Chem. 9 (2009) 66–76.
[22] K.G. Petrov, Y.M. Zhang, M. Carter, G.S. Cockerill, S. Dickerson, C.A. Gauthier, Y. Guo, R.A. Mook, D.W. Rusnak, A.L. Walker, Optimization and SAR for dual ErbB-1/ErbB-2 tyrosine kinase inhibition in the 6-furanylquinazoline series, Bioorg. Med. Chem. lett. 16 (2006) 4686–4691.
[23] H.J. Ross, G.R. Blumenschein, J. Aisner, N. Damjanov, A. Dowlati, J. Garst, J.R. Rigas, M. Smylie, H. Hassani, K.E. Allen, Randomized phase II multicenter trial of two schedules of lapatinib as first-or second-line monotherapy in patients with advanced or metastatic non–small cell lung cancer, Clin. Cancer Res. 16 (2010) 1938–1949.
[24] D.B. Mendel, A.D. Laird, X. Xin, S.G. Louie, J.G. Christensen, G. Li, R.E. Schreck, T.J. Abrams, T.J. Ngai, L.B. Lee, In vivo antitumor activity of SU11248, a novel tyrosine kinase inhibitor targeting vascular endothelial growth factor and platelet-derived growth factor receptors, Clin. Cancer Res. 9 (2003) 327–337.
[25] V.G. Pawar, M.L. Sos, H.B. Rode, M. Rabiller, S. Heynck, W.A. Van Otterlo, R.K. Thomas, D. Rauh, Synthesis and biological evaluation of 4-anilinoquinolines as potent inhibitors of epidermal growth factor receptor, J. Med. Chem. 53 (2010) 2892–2901.
[26] K. Kobayashi, K. Hagiwara, Epidermal growth factor receptor (EGFR) mutation and personalized therapy in advanced nonsmall cell lung cancer (NSCLC), Target. Oncol. 8 (2013) 27–33.
[27] M.M. Ghorab, M.S. Alsaid, A.M. Soliman, A.A. Al-Mishari, Benzo [g] quinazolin-based scaffold derivatives as dual EGFR/HER2 inhibitors, J. Enzyme Inhib. Med. Chem. 33 (2018) 67–73.
[28] M.S. Alsaid, A.A. Al-Mishari, A.M. Soliman, F.A. Ragab, M.M. Ghorab, Discovery of Benzo [g] quinazolin benzenesulfonamide derivatives as dual EGFR/HER2 inhibitors, Eur. J. Med. Chem. 141 (2017) 84–91.
[29] M.M. Ghorab, M.S. Alsaid, A.M. Soliman, F.A. Ragab, VEGFR-2 inhibitors and apoptosis inducers: synthesis and molecular design of new benzo [g] quinazolin bearing benzenesulfonamide moiety, J. Enzyme Inhib. Med. Chem. 32 (2017) 893–907.
[30] D.A.A. El Ella, M.M. Ghorab, H.I. Heiba, A.M. Soliman, Synthesis of some new thiazolopyrane and thiazolopyranopyrimidine derivatives bearing a sulfonamide moiety for evaluation as anticancer and radiosensitizing agents, Med. Chem. Res. 21 (2012) 2395–2407.
[31] H. Hidaka, Y. Sasaki, T. Tanaka, T. Endo, S. Ohno, Y. Fujii, T. Nagata, N-(6-aminohexyl)-5-chloro-1-naphthalenesulfonamide, a calmodulin antagonist, inhibits cell proliferation, Proc. Natl. Acad. Sci. 78 (1981) 4354–4357.
[32] Y. Liu, N.S. Gray, Rational design of inhibitors that bind to inactive kinase conformations, Nat. Chem. Biol. 2 (2006) 358–364.
[33] M. McTigue, B.W. Murray, J.H. Chen, Y.L. Deng, J. Solowiej, R.S. Kania, Molecular conformations, interactions, and properties associated with drug efficiency and clinical performance among VEGFR TK inhibitors, Proc. Natl. Acad. Sci. (2012) 201207759.
[34] J. Stamos, M.X. Sliwkowski, C. Eigenbrot, Structure of the epidermal growth factor receptor kinase domain alone and in complex with a 4-anilinoquinazoline inhibitor, J. Biol. Chem. 277 (2002) 46265–46272.
[35] Z. Tang, S. Niu, F. Liu, K. Lao, J. Miao, J. Ji, X. Wang, M. Yan, L. Zhang, Q. You, Synthesis and biological evaluation of 2, 3-diaryl isoquinolinone derivatives as anti-breast cancer agents targeting ERα and VEGFR-2, Bioorg. Med. Chem. Lett. 24 (2014) 2129–2133.
[36] S. Kamath, J.K. Buolamwini, Targeting EGFR and HER-2 receptor tyrosine kinases for cancer drug discovery and development, Med. Res. Rev. 26 (2006) 569–594.
[37] S. Yakaiah, P.S.V. Kumar, P.B. Rani, K.D. Prasad, P. Aparna, Design, synthesis and biological evaluation of novel pyrazolo-oxothiazolidine derivatives as anti-proliferative agents against human lung cancer cell line A549, Bioorg. Med. Chem. Lett. 28 (2018) 630–636.